Electron Spin Resonance and Mössbauer Evidence for the Trianion $[Fe_2S_2\{(SCH_2)_2C_6H_4\text{-}o\}_2]^{3-}$ †

Peter Beardwood and John F. Gibson *
Department of Chemistry, Imperial College of Science and Technology, London SW7 2AY
Charles E. Johnson and James D. Rush
Department of Physics, Oliver Lodge Laboratory, Oxford Street, P.O. Box 147, Liverpool L69 3BX

Dimethylformamide solutions of $[NEt_4]_2[Fe_2S_2\{(SCH_2)_2C_6H_4\text{-}o\}_2]$ may be reduced at −50 °C using monosodium acenaphthylenide, to give paramagnetic solutions believed to contain the trianion $[Fe_2S_2\{(SCH_2)_2C_6H_4\text{-}o\}_2]^{3-}$ in 60—80% yield. The evidence for this is as follows: the e.s.r. spectrum of a sample enriched in ^{57}Fe was well simulated on this assumption; the *g* values of 2.007, 1.940, and 1.922, the ^{57}Fe hyperfine splittings of 1.52 and 1.35 mT for the two iron atoms, and the variation in linewidth with temperature are quite compatible with published data for reduced two-iron ferredoxins; the Mössbauer spectrum gives clear evidence of antiferromagnetically coupled components of a paramagnetic species closely resembling those found in reduced two-iron ferredoxins. A comparison is made between these results and those of other workers.

The dianion $[Fe_2S_2\{(SCH_2)_2C_6H_4\text{-}o\}_2]^{2-}$ and analogous $[Fe_2S_2(SR)_4]^{2-}$ (R = C_6H_5, *p*-ClC_6H_4, or *p*-MeC_6H_4), originally synthesised by Holm and co-workers,[1,2] have proven to be excellent analogues of the oxidised forms of 2Fe2S proteins.[3,4] Unlike the proteins however, one-electron reduction of these synthetic analogues to a spectroscopically observable $[Fe_2S_2(SR)_4]^{3-}$ species has not been easy although this reaction and a subsequent one-electron reduction to the tetra-anion has been demonstrated polarographically.[2] For $[Fe_2S_2(SPh)_4]^{2-}$ it has been shown that electrochemical reduction to the tri-anion is followed by a facile dimer-to-tetramer $\{[Fe_4S_4(SPh)_4]^{2-}\}$ conversion, and a similar dimerisation process was suggested for $[Fe_2S_2\{(SCH_2)_2C_6H_4\text{-}o\}_2]^{3-}$, although at a slower rate.[5]

Although previous attempts at chemical reduction of $[Fe_2S_2(SR)_4]^{2-}$ complexes have failed to allow subsequent spectral detection of trianion species,[6] it is our experience that with strictly anaerobic conditions the $[Fe_2S_2(SR)_4]^{3-}$ anion is sufficiently stable in mobile solution to allow generation of adequate concentrations, which may then be completely stabilised by immobilisation upon freezing the solvent. Since this work was completed, Mascharak *et al.*[7] have reported their chemical reduction of this dianion which we comment on later.

Experimental

The compound $[NEt_4]_2[Fe_2S_2\{(SCH_2)_2C_6H_4\text{-}o\}_2]$ was prepared from $[NEt_4][Fe\{(SCH_2)_2C_6H_4\text{-}o\}_2]$ [8] by reaction with sodium hydrogensulphide in methanol [5] and obtained as an analytically pure salt, although containing a trace amount of paramagnetic impurity [3] with a weak solution e.s.r. signal at $g \simeq 2.01$ which disappeared on reduction. The dimer was also synthesised on a small scale enriched to 83% in ^{57}Fe.

Reductions were performed anaerobically in dmf (*NN*-dimethylformamide) or dmso (dimethyl sulphoxide) with monosodium acenaphthylenide, generated in dmf solution from acenaphthylene reduced over 0.1—0.2% sodium–mercury amalgam.

In a typical reduction 5 cm^3 of a filtered solution, about 0.5—3 mmol dm^{-3} in iron cluster, was transferred to a septum-capped Schlenk tube and further deoxygenated by several evacuation freeze-thaw dinitrogen flush cycles. An e.s.r. sample tube or Mössbauer cell, well flushed with dinitrogen, was assembled on a stainless steel or Teflon transfer tube inserted into the Schlenk-tube septum ready for immediate transfer of part of the cluster solution subsequent to reduction. In the case of dmf the cluster solution was again frozen at this stage and thawed to around −50 °C just prior to addition of reducing agent. An approximate 1.5-fold excess of monosodium acenaphthylenide in solvent (*ca.* 100 μl) was then added to the dimer solution from a syringe, rapidly mixed by swirling the solution in the Schlenk tube, and an aliquot immediately transferred to the sample holder where it was quickly frozen in liquid nitrogen. With experience, the whole process from addition of reducing agent to completion of solvent solidification could be performed in 15—20 s. The reaction is accompanied by a change in colour from dark brown-grey to a light tan and a visible spectrum recorded after several minutes at room temperature shows gross diminution of all features characteristic of $[Fe_2S_2\{(SCH_2)_2C_6H_4\text{-}o\}_2]^{2-}$.

Instrumentation.—Electron spin resonance measurements were made with a Varian E12 spectrometer operating at *ca.* 9.15 GHz. Samples were cooled in a stream of nitrogen gas, the temperature of which was regulated by a Varian variable temperature accessory. The e.s.r. spectral simulations were performed by spatial integration using a modified version of a program originally written by White and Belford,[9] incorporating the additional transition probability correction factor $(1/g)$.[10] The linewidth anisotropy was linearly interpolated by field between values set at the *g* extrema. Best fits to the experimental spectra were achieved by minimisation of summed squared-differences. Mössbauer measurements were obtained with sources of ^{57}Co in palladium and ^{57}Co in rhodium. An absorber of pure iron was used for calibration and the spectra were plotted with the centre of the iron spectrum as zero velocity. A superconducting solenoid was used to provide the high magnetic fields perpendicular to the γ-ray beam.

Results and Discussion

E.S.R. Studies.—Figure 1(*a*) shows a typical e.s.r. spectrum recorded at *ca.* 100 K. In this case the dmf solvent contains $[NBu^n_4][ClO_4]$ (0.1 mol dm^{-3}) which has the effect of yielding a true transparent glass on freezing although this is observed

† Di-μ-sulphido-bis[*o*-xylene-α,α′-dithiolatoferrate](3−).

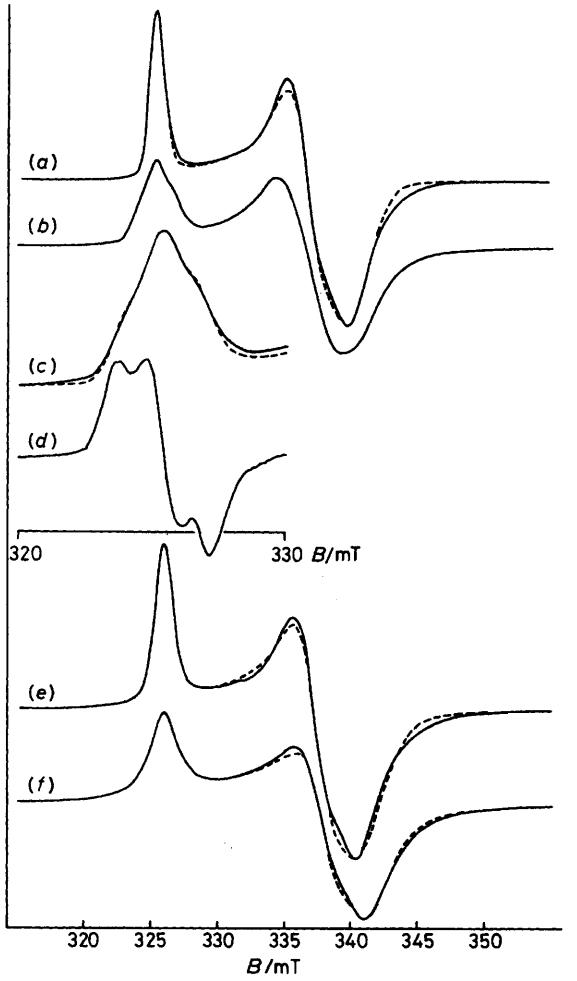

Figure 1. Electron spin resonance spectra (——), together with simulations (– – – –) of the trianion $[Fe_2S_2\{(SCH_2)_2C_6H_4\text{-}o\}_2]^{3-}$: (*a*) with naturally occurring Fe and (*b*) with 83% ^{57}Fe enrichment, at 100 K in dmf containing 0.1 mol dm^{-3} $[NBu^n_4][ClO_4]$ (microwave frequency 9.142 GHz, microwave power 2 mW); (*c*) the low-field feature of (*b*), (*d*) the second derivative of the low-field feature of (*b*), (*e*) in dmso, at 100 K, and (*f*) at 190 K (9.160 GHz, 50 mW)

to devitrify at higher temperatures yielding a broader line. With pure dmf or dmso crystallisation and line broadening occur directly on freezing [Figure 1(*e*)]. The production of the narrowest linewidth possible becomes especially important to the analysis of the first and second derivative e.s.r. lineshapes for the reduced sample of 83% ^{57}Fe enriched $[Fe_2S_2\{(SCH_2)_2C_6H_4\text{-}o\}_2]^{2-}$, depicted in Figure 1(*b*). To high field in this Figure only an overall broadening results from ^{57}Fe enrichment; for the low-field peak, side shoulders are apparent and in the second-derivative lineshape a splitting is seen quite clearly [Figure 1(*d*)]. With the level of isotopic enrichment employed, the spectrum resulting from a spin-coupled iron(II)–iron(III) dimer is expected to possess three component spectra. For iron sites having equivalent nuclear hyperfine interactions the majority of the sample (69%), containing two ^{57}Fe ions, will give rise to a 1 : 2 : 1 triplet for the low-field peak.[11] The substantial proportion of mixed ^{56}Fe–^{57}Fe dimers (28%) will result in a splitting to a doublet and the remaining small fraction will appear similar to the unenriched spectrum. By field-shifting the spectrum for the natural abundance ^{56}Fe sample with the ^{57}Fe hyperfine splitting, and adding component spectra according to the expected statistical distribution for the three isotopic mixtures, it is possible to obtain a good fit to the low-field peak of the ^{57}Fe enriched spectral lineshape. A least-squares fitting procedure leads to an estimated hyperfine splitting of 1.4 mT. If the splittings produced by iron(II) and iron(III) sites are allowed to be inequivalent, values of 1.52 (43) and 1.35 mT (38 MHz) achieve the best fit [Figure 1(*c*)]. The splitting, assuming equivalent hyperfine interactions from the two irons, is quite compatible with the value of 1.4 mT obtained from putidaredoxin [12] and spinach ferredoxin [13] by a similar method and 1.5 mT found for parsely ferredoxin.[14] ENDOR measurements for several 2Fe2S proteins have indicated effective splittings of *ca.* 1.2—1.3 and 1.4—1.5 mT along the hyperfine tensor *z* axis for iron(II) and iron(III) sites respectively.[15,16]

Measured *g* values from the maximum, crossover, and minimum of the unenriched spectrum are 2.007, 1.940, and 1.922 respectively such that the average *g* value is significantly below 2.0, in keeping with the antiferromagnetic coupling model of Gibson *et al.*,[17] applicable to 2Fe2S ferredoxins. Overall, the spectrum is better simulated with a Gaussian rather than Lorentzian convolution lineshape, however, neither is entirely adequate. The least-squares fitted calculated line in Figure 1(*a*) results from the use of a mixed Gaussian–Lorentzian convolution product according to the parameters in Table 1, but still leads to an inadequate fit to the high-field half of the spectrum.

The principal axis *g* values are quite similar to those observed for the two-iron ferredoxins from *Azotobacter vinelandii* [18] and *Clostridium pasteurianum* [19] or to those for adrenodoxin and putidaredoxin [15] (Table 1). Furthermore, the *g* values are in excellent agreement with the analysis of Bertrand and Gayda [20] whereby variations in *g* values amongst a wide range of two-iron ferredoxins may be understood in terms of a variable degree of rhombic distortion at the iron(II) site. It is also interesting to note that the *g*-value extrema measured by Cammack and co-workers [21–23] for several unfolded proteins, wherein the iron–sulphur chromophore is artificially exposed to the solvent, move toward those observed here for $[Fe_2S_2\{(SCH_2)_2C_6H_4\text{-}o\}_2]^{3-}$.

The behaviour of the e.s.r. signal with changing temperature is entirely consistent with that expected for $[Fe_2S_2\{(SCH_2)_2C_6H_4\text{-}o\}_2]^{3-}$. At *ca.* 100 K the spectrum is readily observable and difficult to power-saturate. On cooling to *ca.* 10 K a very similar lineshape is observed but the signal easily saturates. At such low temperatures one would expect to find evidence of any reduced tetrameric species which might have resulted from dimerisation of trianionic dimers followed by further reduction by excess acenaphthylenide; [5] we could find none. Spectra measured at temperatures in the region of 200 K show greatly increased linewidth and a Lorentzian lineshape [Figure 1(*f*), Table 1] in keeping with a faster relaxation process, but this is still slower than that of some iron-sulphur proteins [24] measured at lower temperatures. With non-vitreous samples, for which no change in solvent structure concomitant with line broadening is found at higher temperatures, this linewidth temperature-dependency is reversible.

For e.s.r. signals obtained by reduction at low temperatures in dmf, comparison of doubly integrated intensities with a copper(II) ethylenediaminetetra-acetate standard indicates 60—80% yield of the trianion in the majority of reductions. The signal intensities of such solutions, measured at 100 K, were observed to have decayed completely after 2—3 min at 20 °C. At −50 °C, on the other hand, solutions of *ca.* 0.5 mmol dm^{-3} in $[Fe_2S_2\{(SCH_2)_2C_6H_4\text{-}o\}_2]^{3-}$ had greatly increased stability such that the e.s.r. signal intensity measured at 100 K decreased only slightly over a period of a few hours in the strict absence of molecular oxygen. For these reasons reductions effected in dmso led to only *ca.* 20% yield of trianion as

Table 1. E.s.r. data of the trianion $[Fe_2S_2\{(SCH_2)_2C_6H_4\text{-}o\}_2]^{3-}$ in various conditions compared with those of the iron clusters in some reduced ferredoxins

	Parameter	*z*	*y*	*x*
(*a*) Conditions for $[Fe_2S_2\{(SCH_2)_2C_6H_4\text{-}o\}_2]^{3-}$				
In dmf (0.1 mol dm^{-3} $[NBu^n_4][ClO_4]$) at 100 K [a]	Measured *g* values	2.007	1.940	1.922
	Simulated *g* values	2.006	1.939	1.919
	Gaussian widths [b]/mT	0.55	1.24	1.42
	Lorentzian widths [b]/mT	0.15	0.32	0.42
In dmso at 100 K [c]	Measured *g* values	2.008	1.940	1.923
	Simulated *g* values	2.008	1.940	1.919
	Gaussian widths [b]/mT	0.58	1.02	1.42
	Lorentzian widths [b]/mT	0.4	0.91	0.98
In dmso at 190 K [d]	Measured *g* values	2.007	1.939	1.918
	Simulated *g* values	2.008	1.937	1.916
	Lorentzian widths [b]/mT	1.24	1.81	2.05
(*b*) Reduced ferredoxin				
Adrenodoxin [e]	Measured *g* values	2.02	1.935	1.93
Putidaredoxin [e]		2.02	1.935	1.93
Clostridium pasteurianum [f]		2.00	1.95	1.93
Azotobacter vinelandii I [g]		2.009	1.941	1.917

[a] As in Figure 1(*a*). [b] Half width at half height. [c] As in Figure 1(*e*). [d] As in Figure 1(*f*). [e] Ref. 15. [f] Ref. 19. [g] Ref. 18.

of necessity they were performed above the solvent freezing point of 18 °C.

Mössbauer Studies.—The dianion. Synthesis of $[Fe_2S_2\{(SCH_2)_2C_6H_4\text{-}o\}_2]^{2-}$ enriched in ^{57}Fe has permitted the measurement of solution Mössbauer spectra before and after reduction. Figure 2 shows low temperature spectra for a frozen dmf solution of the dianion in zero applied field and with fields of 3, 6, and 10 T applied perpendicular to the γ-ray beam. The zero-field spectrum appears very similar at 77 K. Spectra for the dianion may be characterised by 1 : 1 addition of two spectra having slightly different quadrupole splittings. Inequivalence in the splittings for the two iron(III) sites is revealed in the zero-field spectrum by a linewidth rather larger than the instrumental linewidth. Mössbauer spectra of some oxidised two-iron ferredoxins also show inequivalence between the two irons.[16,25] The absence of an observable hyperfine field is in keeping with antiparallel coupling of the spins for the two iron(III) ions to give a singlet ground state. Table 2 lists spectral parameters deduced from fitting the calculated lineshapes shown in Figure 2. These compare quite favourably with values derived from Mössbauer spectra of 2Fe2S ferredoxins,[16,26–30] although the quadrupole splitting (ΔE_Q) values are smaller than those found for the proteins. The reversed sign for this parameter is not particularly significant because the electric field gradient is very sensitive to small disturbances from cubic symmetries and can usually be of either sign; it is also likely to be temperature dependent.

It is interesting to compare the parameters found for $[Fe_2S_2\{(SCH_2)_2C_6H_4\text{-}o\}_2]^{2-}$ in frozen solution with those measured for crystalline salts containing the same ion. For the polycrystalline materials having NEt_4^+ or $AsPh_4^+$ cations, δ (isomer shift) = +0.17 mm s^{-1}, ΔE_Q = 0.36 mm s^{-1}, and Γ = 0.30 mm s^{-1} with rigorous equivalence between the two iron atoms.[2,4] Thus, we find that the dianion more closely resembles the protein 2Fe2S site when it is in frozen solution than when in a crystalline environment. Incidentally, the isomer shift calculated using the crystallographic data for $[NEt_4]_2[Fe_2S_2\{(SCH_2)_2C_6H_4\text{-}o\}_2]$ and the empirical equations of Hoggins and Steinfink [31] is 0.27 mm s^{-1} in striking agreement with the values we find for the solution (Table 1).

The trianion. Figure 3 shows Mössbauer spectra observed in applied fields at 4.2 K for $[Fe_2S_2\{(SCH_2)_2C_6H_4\text{-}o\}_2]^{2-}$ after reduction in dmf with acenaphthylenide. With a field of only 0.25 T perpendicular to the γ-ray beam the presence of a paramagnetic species is clearly seen together with a doublet characteristic of the dianion. This spectrum and those measured at the high applied fields may be quite well fitted by a procedure involving addition of calculated spectra corresponding to an antiferromagnetically coupled iron(III)–iron(II) pair together with a proportion (40%) of the di-iron(III) complex as simulated in the pre-reduced state. Iron(III) and iron(II) components of the paramagnetic species are seen most clearly in the simulation for the 0.25 T spectrum. The sharper spectrum resulting from the iron(III) and giving rise to most of the absorption at 3.2 mm s^{-1} exhibits a decreased hyperfine splitting at higher applied fields whilst the broader iron(II) component is observed to develop increased splitting and is responsible for the absorption at *ca.* 4.4 mm s^{-1} in a 10 T field. This behaviour demonstrates plurality of magnetically inequivalent sites with negative and positive hyperfine fields respectively and is typical of the antiparallel spin-coupled 2Fe2S site in reduced two-iron ferredoxins. Parameters relevant to the simulations in Figure 3 are given in Table 3 and are comparable to those for the proteins.[16,28–30] The average of the *z* axis hyperfine splittings from iron(II) and iron(III) nuclei is quite comparable with that estimated from simulation of the ^{57}Fe enriched e.s.r. spectrum (Table 1).

For Mössbauer spectra measured with magnetic fields applied parallel to the γ-ray beam there is evidence for a small amount of absorption in addition to that from dianion and trianion dimers. The species causing this appears paramag-

Table 2. Mössbauer spectral parameters of the dianion $[Fe_2S_2\{(SCH_2)_2(C_6H_4\text{-}o\}_2]^{2-}$ taken at 4.2 K compared with those of some typical 2Fe2S ferredoxins in their oxidised forms

	$[Fe_2S_2\{(SCH_2)_2C_6H_4\text{-}o\}_2]^{2-}$		Typical ferredoxin [a]
	Site 1	Site 2	
δ [b]/mm s^{-1}	+0.27	+0.29	+0.2 to +0.3
ΔE_Q/mm s^{-1}	−0.40	−0.57	0.6—0.8
η [c]	0.6	0.6	0.4—0.5
Γ [d]/mm s^{-1}	0.30	0.30	

[a] Refs. 16, 26, 27, 29, 30 (data taken at 4.2 K and higher temperatures) and 28 (data taken at 195 K). [b] Relative to Fe metal. [c] Asymmetry parameter. [d] Full width at half height.

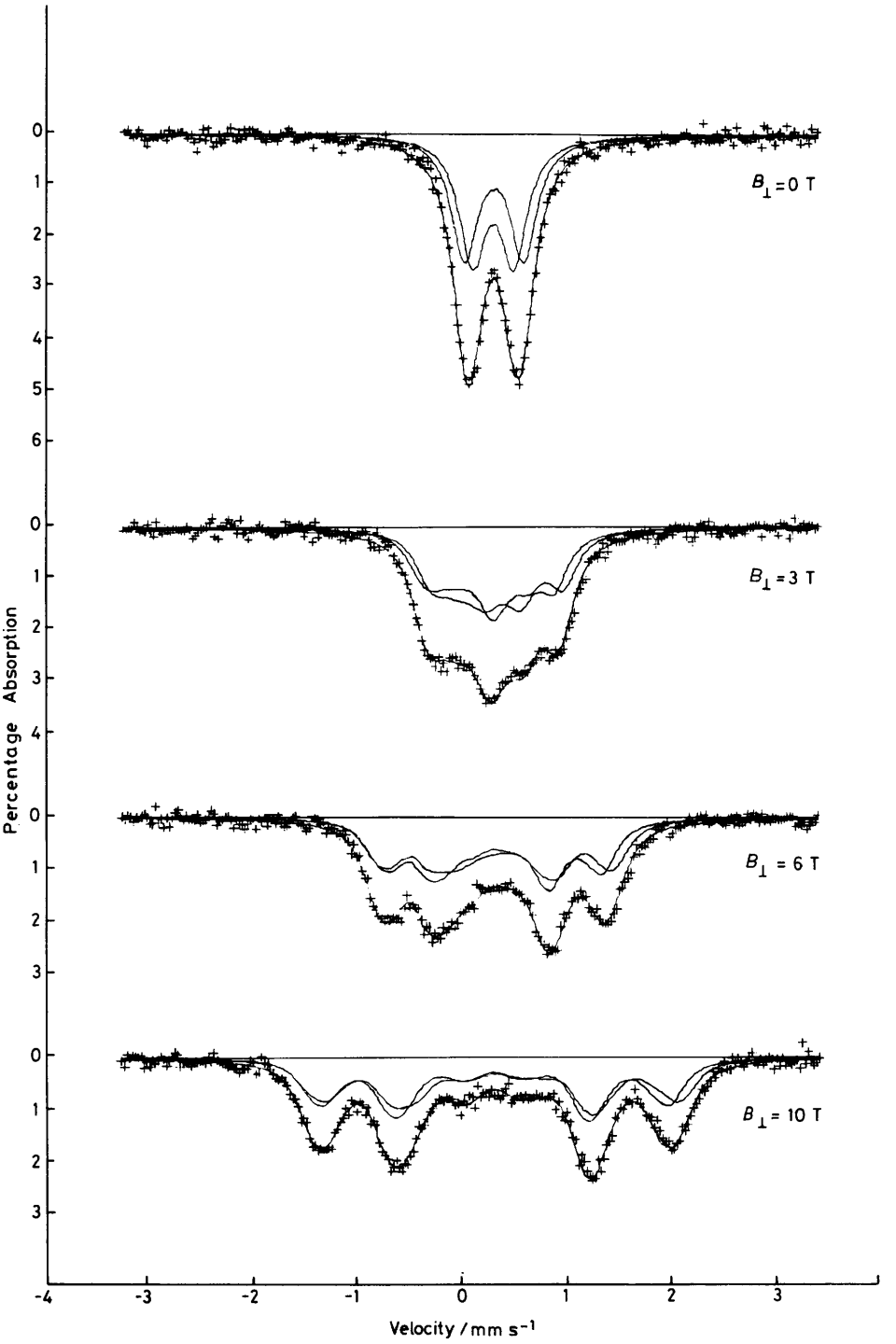

Figure 2. Mössbauer spectra of $[NEt_4]_2[Fe_2S_2\{(SCH_2)_2C_6H_4\text{-}o\}_2]$ (0.6 mmol dm^{-3}) in dmf at 4.2 K with varying fields applied perpendicular to the γ-ray beam

netic and possibly results from decomposition or further reaction of $[Fe_2S_2\{(SCH_2)_2C_6H_4\text{-}o\}_2]^{3-}$. However, a sample deliberately thawed and held at room temperature for several minutes was not helpful in the diagnosis since although it showed a radically different low temperature Mössbauer spectrum, this could not readily be interpreted in terms of any likely product, such as a tetrameric iron–sulphur cluster. Alternatively, the unexplained absorption could genuinely arise from the trianion species but not be simulated successfully if, for example, the effective field at the iron nuclei is not parallel to the applied field as has been assumed in our simulation program. Thus, this absorption does not necessarily arise from an impurity. If it did it would represent about 10% of the iron present.

Mascharak *et al.*[7] have already reported the e.s.r. spectrum we show in Figure 1(*a*), but since their Mössbauer spectrum is

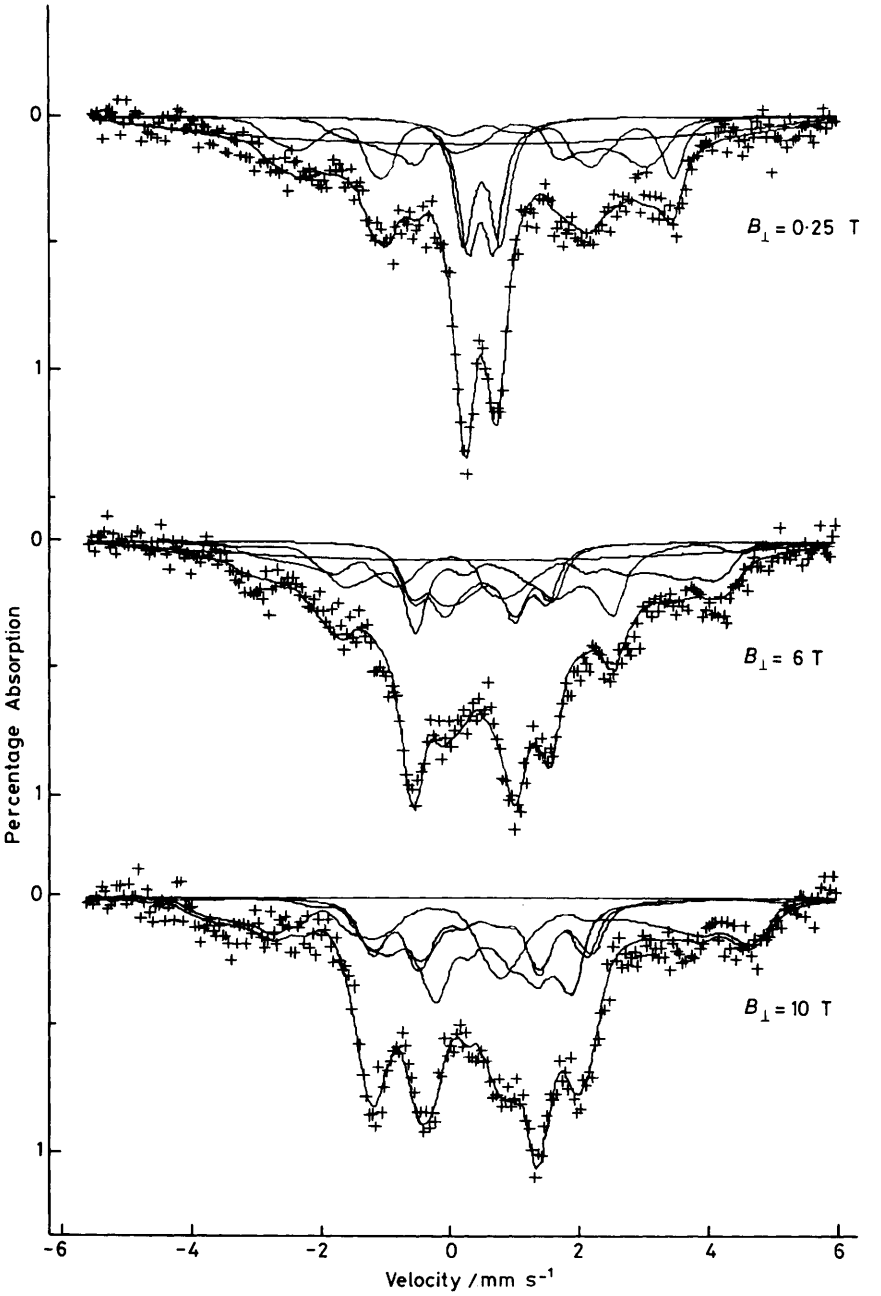

Figure 3. Mössbauer spectra of $[NEt_4]_2[Fe_2S_2\{(SCH_2)_2C_6H_4\text{-}o\}_2]$ (0.6 mmol dm^{-3}) in dmf at 4.2 K after reduction with a two-fold excess of monosodium acenaphthylenide. The magnetic field was applied perpendicular to the γ-ray beam

different from ours (Figure 3) some comment is called for. From our experience that the e.s.r. signal of the trianion disappears within a few minutes at room temperature in our solvent (dmf) we are sceptical about using reaction times of 45 min for e.s.r. or 4.5 h for Mössbauer even though more concentrated solutions in a different solvent were used. In fact, a crude calculation allowing for the different spectrometer conditions used leads us to the conclusion that the 80 K e.s.r. signal of Mascharak *et al.*[7] represents no more than about 1% of the total iron present. This is in keeping with their observation of other paramagnetic species, with the possibility of the formation of diamagnetic species and/or tetramers and of incomplete reduction. Also, we draw attention to the Mössbauer spectrum, Figure 5(*b*), of Mascharak *et al.*[7] and note that although it is similar to those of typical reduced ferredoxin proteins it corresponds to a fast relaxing protein, yet the sample was at 4.2 K. Note that their e.s.r. spectrum even at 80 K is not relaxing fast. Thus, there is an incompatibility between their e.s.r. and their Mössbauer data; the spectra could not arise from the same species. Our sample which gave the Mössbauer spectra of Figure 3 also gave a Mössbauer spectrum with magnetic hyperfine structure at 77 K thus showing slow relaxation in keeping with the well resolved e.s.r. spectrum at that temperature. Furthermore, we would add that the u.v.–visible spectrum assigned to the trianion and recorded in Figure 2 of ref. 7 does not necessarily arise from that species because in our hands, although acenaphthylenide reduction of the dianion gives a solution with much the same

Table 3. Mössbauer spectral parameters of the trianion $[Fe_2S_2\{(SCH_2)_2C_6H_4\text{-}o\}_2]^{3-}$ taken at 4.2 K compared with those of some typical 2Fe2S ferredoxins in their reduced form

	$[Fe_2S_2\{(SCH_2)_2C_6H_4\text{-}o\}_2]^{3-}$		Typical ferredoxins [a]	
	Fe^{3+}	Fe^{2+}	Fe^{3+}	Fe^{2+}
δ [b]/mm s^{-1}	+0.33	+0.7	+0.15 to +0.3	+0.40 to +0.55
ΔE_Q/mm s^{-1}	−0.7	+3.0	+0.6 to +0.8	−2.5 to −3.2
η [c]	0.65	0.35	−0.3 to −0.9	0.0
Γ [d]/mm s^{-1}	0.31			
A_x [e]/mT	−2.0	0.4	−1.93 to −2.06	0.42—0.52
A_y [e]/mT	−1.7	0.3	−1.7 to −1.85	0.51—0.78
A_z [e]/mT	−1.8	1.4	−1.46 to −1.53	1.17—1.27
A_z [f]/mT	|1.52|	|1.35|		

[a] Refs. 16, 29, 30 (data at 4.2 K) and 28 (data at 195 K). [b] Relative to Fe metal. [c] Asymmetry parameter. [d] Full width at half height. [e] Hyperfine tensor from Mössbauer. [f] Hyperfine tensor from e.s.r.

u.v.–visible spectrum, it was, after such a long time at room temperature, *not* then e.s.r.-active.

We conclude from this comparison that great care must be taken in repeating this work since the desired product is very reactive, and that while the e.s.r. spectrum of Mascharak *et al.*[7] is believed to be that of $[Fe_2S_2\{(SCH_2)_2C_6H_4\text{-}o\}_2]^{3-}$, the Mössbauer spectrum is not. We do not disagree with the major conclusion of their paper, that discrete Fe^{2+} and Fe^{3+} sites exist in the trianion since we observe these in our Mössbauer spectra.

Conclusion

We conclude from the above spectroscopic results that a substantial proportion of $[Fe_2S_2\{(SCH_2)_2C_6H_4\text{-}o\}_2]^{3-}$ may be observed following chemical reduction of $[Fe_2S_2\{(SCH_2)_2C_6H_4\text{-}o\}_2]^{2-}$ in solution using a fairly simple technique of reaction and product capture. As expected, the trianion exhibits characteristics closely matching those of reduced 2Fe2S ferredoxins. Future work will involve more detailed description of the e.s.r. properties of this species.

References

1 J. J. Mayerle, R. B. Frankel, R. H. Holm, J. A. Ibers, W. D. Phillips, and J. F. Weiher, *Proc. Natl. Acad. Sci. USA*, 1973, **70**, 2429.
2 J. J. Mayerle, S. E. Denmark, B. V. DePamphilis, J. A. Ibers, and R. H. Holm, *J. Am. Chem. Soc.*, 1975, **97**, 1032.
3 W. O. Gillum, R. B. Frankel, S. Foner, and R. H. Holm, *Inorg. Chem.*, 1976, **15**, 1095.
4 B-K. Teo, R. G. Shulman, G. S. Brown, and A. E. Meixner, *J. Am. Chem. Soc.*, 1979, **101**, 5624.
5 J. Cambray, R. W. Lane, A. G. Wedd, R. W. Johnson, and R. H. Holm, *Inorg. Chem.*, 1977, **16**, 2565.
6 B. A. Averill, J. R. Bale, and W. H. Orme-Johnson, *J. Am. Chem. Soc.*, 1978, **100**, 3034.
7 P. K. Mascharak, G. C. Papaefthymiou, R. B. Frankel, and R. H. Holm, *J. Am. Chem. Soc.*, 1981, **103**, 6110.
8 R. W. Lane, J. A. Ibers, R. B. Frankel, and R. H. Holm, *Proc. Natl. Acad. Sci. USA*, 1975, **72**, 2868.
9 L. K. White and R. L. Belford, *J. Am. Chem. Soc.*, 1976, **98**, 4428.
10 R. Aasa and T. Vänngård, *J. Magn. Reson.*, 1975, **19**, 308.
11 C. E. Johnson, R. Cammack, K. K. Rao, and D. O. Hall, *Biochem. Biophys. Res. Commun.*, 1971, **43**, 564.
12 J. C. M-Tsibris, R. L. Tsai, I. C. Gunsalus, W. H. Orme-Johnson, R. E. Hansen, and H. Beinert, *Proc. Natl. Acad. Sci. USA*, 1968, **59**, 959.
13 G. Palmer, *Biochem. Biophys. Res. Commun.*, 1967, **27**, 315.
14 J. A. Fee and G. Palmer, *Biochim. Biophys. Acta*, 1971, **245**, 175.
15 J. Fritz, R. Anderson, J. Fee, G. Palmer, R. H. Sands, J. C. M. Tsibris, I. C. Gunsalus, W, H. Orme-Johnson, and H. Beinert, *Biochim. Biophys. Acta*, 1971, **253**, 110.
16 R. E. Anderson, W. R. Dunham, R. H. Sands, A. J. Bearden, and H. L. Crespi, *Biochim. Biophys. Acta*, 1975, **408**, 306.
17 J. F. Gibson, D. O. Hall, J. H. M. Thornley, and F. R. Whatley, *Proc. Natl. Acad. Sci. USA*, 1966, **56**, 987.
18 D. V. Dervartanian, Y. I. Shethna, and H. Beinert, *Biochim. Biophys. Acta*, 1979, **194**, 548.
19 H. Brintzinger, G. Palmer, and R. H. Sands, *Proc. Natl. Acad. Sci. USA*, 1966, **55**, 397.
20 P. Bertrand and J-P. Gayda, *Biochim. Biophys. Acta*, 1979, **579**, 107.
21 R. Cammack, *Biochem. Soc. Trans.*, 1975, **3**, 482.
22 R. Cammack, K. K. Rao, and D. O. Hall, *Biochem. Biophys. Res. Commun.*, 1971, **44**, 8.
23 L. Kerscher, D. Oesterhelt, R. Cammack, and D. O. Hall, *Eur. J. Biochem.*, 1976, **71**, 101.
24 J-P. Gayda, J. F. Gibson, R. Cammack, D. O. Hall, and R. Mullinger, *Biochim. Biophys. Acta*, 1976, **434**, 154.
25 M. M. Werber, E. R. Bauminger, S. G. Cohen, and S. Ofer, *Biophys. Struct. Mech.*, 1978, **4**, 169.
26 R. Cammack, K. K. Rao, D. O. Hall, and C. E. Johnson, *Biochem. J.*, 1971, **125**, 849.
27 C. E. Johnson, E. Elstner, J. F. Gibson, G. Benfield, M. C. W. Evans, and D. O. Hall, *Nature (London)*, 1968, **220**, 1291.
28 K. K. Rao, R. Cammack, D. O. Hall, and C. E. Johnson, *Biochem. J.*, 1971, **122**, 257.
29 E. Munck, P. E. Debrunner, J. C. M. Tsibris, and I. C. Gunsalus, *Biochemistry*, 1972, **11**, 855.
30 W. R. Dunham, A. J. Bearden, I. T. Salmeen, G. Palmer, R. H. Sands, W. H. Orme-Johnson, and H. Beinert, *Biochim. Biophys. Acta*, 1971, **253**, 134.
31 J. T. Hoggins and H. Steinfink, *Inorg. Chem.*, 1976, **15**, 1682.

Received 8*th March* 1982; *Paper* 2/399